Desalination and Water Treatment
www.deswater.com

doi: 10.5004/dwt.2020.26224

203 (2020) 238–253
November

Single and dual fixed-bed columns for the removal of Cd(II) and Ni(II) from water using volcanic rocks: application of Box–Behnken design

Esayas Alemayehu[a,b,*], Perumal Asaithambi[a,*], Bernd Lennartz[c]

[a]*Faculty of Civil and Environmental Engineering, Jimma Institute of Technology, Jimma University, P.O. Box: 378 Jimma, Ethiopia, Tel. +251 472115547; Fax: +251 471111450; emails: esayas16@yahoo.com (E. Alemayehu), drasaithambi2014@gmail.com (P. Asaithambi)*
[b]*Africa Center of Excellence for Water Management, Addis Ababa University, P.O. Box: 1176 Addis Ababa, Ethiopia*
[c]*Institute for Land Use, Rostock University, Justus-Von-Liebig-We 6, 18059 Rostock, Germany*

Received 6 November 2019; Accepted 6 June 2020

ABSTRACT

In this study, a continuous fixed-bed column adsorption system was employed for the removal of Cd(II) and Ni(II) from water using volcanic rocks, virgin pumice (VPum), and virgin scoria (VSco), as adsorbents. The effects of operating parameters such as particle size of adsorbents, initial heavy metal concentrations, flow rates, and media bed type (single and dual) on the adsorption performance of the column were examined at constant bed depth. The adsorption process parameters such as breakthrough time, retardation factors, total removal capacity of the adsorbents for Cd(II), and Ni(II) ions, adsorption exhaustion rate, and breakthrough volume were obtained. When the influent solution was fed to the column at a slow flow rate (Q = 2.5 mL min^{-1}), the breakthrough volume increased significantly compared to the influent solution at a faster flow rate (Q = 5 mL min^{-1}). The influent contained 2 mg L^{-1} Cd(II) and Ni(II), and better than 99% removal was achieved under optimum conditions. Box–Behnken design, a common approach of response surface methodology, was applied to optimize the variables affecting the adsorption of the heavy metals. The quadratic regression models with estimated coefficients were developed and it was observed that model predictions matched with experimental values with an R^2 value of 0.91 and 0.98 for Cd(II) and Ni(II) removal respectively. Relatively higher sorption capacities were observed in dual bed (VSco + VPum) column operation compared to a single bed (VSco) operation. Finally, the results obtained have shown that both volcanic rocks have a high potential for use as a filter bed material in water and wastewater treatment technologies.

Keywords: Adsorptive filter; Box–Behnken design; Breakthrough analysis; Dual media; Heavy metals removal

1. Introduction

The chemical contamination of water from a wide range of toxic derivatives, in particular heavy metals, is a serious environmental problem owing to their potential human toxicity. Heavy metal compounds are widely used in electroplating, metal finishing, leather tanning, wood processing, fertilizers, and so on [1–3]. The significant potential heavy metal sources that pollute the water are industrial activities, random discharge of untreated wastes (solid and liquid) as well as a natural occurrence of heavy metals. Among the most frequently discharged heavy metals from point sources of pollution such as cadmium (Cd) and nickel (Ni) had been recognized as a health hazard for many decades. The presence of Cd and Ni over the permissible levels causes human health problems such as damage to the liver, kidney, and

* Corresponding authors.

1944-3994/1944-3986 © 2020 Desalination Publications. All rights reserved.

lung efficiency, mental deterioration, hypertension, bone degeneration, muscular and cardiovascular disorders, cancer, skin irradiation and damage the nervous system [4–6]. Thus, due to the health effects of high Cd and Ni in water, it is essential to reduce their concentrations to the allowable limits.

A number of technologies have been developed over the year for the removal of Cd and Ni from contaminated water such as conventional treatment technique, membrane separation, precipitation, and ion exchange. However, many of these are suffering from either poor removal efficiency, or high operational and maintenance costs, or availability of raw materials, or generation of toxic sludge difficult to dispose of [7–11]. Among the existing technologies, the adsorption-based process appears to be the most promising method, due to high removal efficiency, ease of operation, and simplicity of design. Although activated carbon is suggested as a competitive and effective adsorbent for the removal of heavy metals, in developing countries naturally occurring and abundantly available adsorbents are receiving significant attention due to their low-cost [12,13].

Natural materials such as rock minerals and soils are considered as a potential remediation agent for the elimination of numerous heavy metals from contaminated water [14–16]. Consequently, many efforts have been employed to have easily accessible, low-cost, and efficient natural adsorbents that may be applied for the treatment of water and wastewater in underdeveloped countries such as Ethiopia. Volcanic rocks (VPum and VSco) are among the most encouraging types of easily accessible and low-cost adsorbents. Previously, we studied the removal of Cd(II) and Ni(II) from water, using these volcanic rock adsorbents under selected conditions in batch mode [17,18]. The rocks reasonably meet the criteria that have been established for water and wastewater treatment processes due to its high natural porosity, very low price, good mechanical resistance, and suitability for pollutant adsorption.

Most of the researches that have been done using natural adsorbents for heavy metals removal is based on batch experimental setups [19,20]. The adsorption capacity of adsorbents gained from the batch experiment is valuable in giving basic information about the effectiveness of the adsorbents. However, the data obtained from batch studies may not be appropriate for continuous processes (fixed-bed column) where insufficient contact time for the achievement of the equilibrium. Consequently, studies by different authors [21–23], reveals that fixed-bed columns is more desirable and industrially feasible for removal of heavy metals from water. Hence, there is an interest to conduct adsorption study in a column mode.

The main objectives of the current work were to investigate the heavy metals mixture [24] sorption capacity of VPum and VSco under fixed-bed column adsorption setup: compare the adsorption properties of both adsorbents with each other; investigate the Cd(II) and Ni(II) adsorption mechanisms with respect to varying initial heavy metal concentration, flow rate, particle size, and media bed type (single and dual) on the performance of breakthrough curves; and the operating parameters were optimized by using multivariate mathematical model approach so-called response surface methodology (RSM).

2. Materials and methods

2.1. Adsorbates solutions

Chemicals used in these investigations such as $CdCl_2H_2O$, $Ni(NO_3)_2{\cdot}6H_2O$, $CaCl_2{\cdot}2H_2O$, KBr, HCl, and NaOH, were analytical reagent grade chemicals from Merck (Darmstadt, Germany). The varying metal concentrations of working solutions were freshly prepared by diluting the stock solution (1,000 mg L^{-1}) for each experimental run. The initial ionic strength of the prepared solutions was adjusted to 0.01 M by adding $CaCl_2{\cdot}2H_2O$ into the solution. All precautions were taken to minimize the loss due to the evaporation during the preparation of solutions and subsequent measurements. The adsorption experiments were carried out at all an optimum pH of 5 ± 0.1 obtained by batch experiments [17,18].

2.2. Adsorbents characterization

Volcanic rocks are found in abundance in Europe (Greece, Spain, Turkey, etc), Central America, Southeast Asia (Vietnam, etc.) and Africa (Ethiopia, Eretria, Djibouti, etc.) [17,19,20]. In this study, the rocks are collected from volcanic cones (VPum: 8°10′N 39°50′E; VSco: 8°33′N 39°16′E) of the Main Rift Valley area of Ethiopia. VPum and VSco are very abundant local volcanic rocks that cover about 1/3 of the country's total area and have a variety of mineralogical and chemical compositions [17,25]. It has been well known that every new purification agent must satisfy the basic characteristics of filter media before it can be considered for use. These concerns its grain size, density, solubility, durability, specific surface area, porosity, and material strength. Accordingly, acid solubility measurement was performed according to AWWA [26]. The measurement was effected under the action of 20% hydrochloric acid. The material loss after 24 h did not exceed 2%. Furthermore, a durability test was conducted by packing the adsorbent in a column and backwashing it for 100 h [27,28]. Besides, material strength was determined by scratching it with the different minerals in the Moh's scale: VSco = 7.0 and VPum = 6.0 obtained. Purity was also tested by the absence of organic matter (heating at 500°C for 24 h). Preparation and characterization of the rock samples were done as reported earlier [17,18]. The temperature of all experiments was at room temperature (25°C–26°C). Granulometric analysis and hydrological parameters are presented in Table 1.

In addition, the crystalline phases of VPum and VSco were characterized by means of X-ray diffraction (XRD) instrumental technique. XRD is a technique used for determining the atomic and molecular structure of a crystal [29]. Accordingly, the mineralogical accumulation of the adsorbents was explained by matching the X-ray diffractogram with the database in Match! 3 software (version 3.8.3.151). As can be seen from supplementary data (Fig. S1) the main crystalline phases in VPum were CaO and SiO_2; and the only SiO_2 for VSco. The detected dome in both samples between at 2θ = 10° and 40° can be considered as an indication for the existence of some amorphous phase. A similar observation has been reported in the XRD analysis of pumice for Cr(VI) removal [19]. In general, VPum and VSco reasonably meet the criteria that have been established for water

Table 1
Granulometric analysis and hydrological parameters

Parameters			VSco				VPum	
Particle size (mm)	0.075–0.425		0.425–2.0		0.075–0.425		0.425–2.0	
m_{ads} (gm)		608.7		532.9		230.6		146.5
ρ_b (gm cm^{-3})		1.24		1.09		0.47		0.30
ρ_s (gm cm^{-3})		2.96		2.85		2.33		2.01
ε		0.58		0.62		0.80		0.85
V_v (cm^3)		283.8		302.6		390.5		416.8
Q (cm^3 min^{-1})	2.5	5	2.5	5	2.5	5	2.5	5
EBCT (min)	195.81	97.91	195.81	97.91	1,995.81	97.91	195.81	97.91
υ (cm min^{-1})	0.013	0.05	0.013	0.05	0.013	0.05	0.013	0.05
ν (cm min^{-1})	0.022	0.086	0.021	0.081	0.016	0.062	0.015	0.059

and wastewater treatment processes due to its high natural porosity, good mechanical resistance, and suitability for pollutant adsorption.

2.3. Experimental setup and procedures

A small scale cylindrical up-flow column with an internal diameter of 8.1 cm, a height of 9.5 cm, and an empty bed volume of 490 cm^3 was used (Fig. 1). To avoid air bubbles, the column was carefully packed underwater. The adsorbent in the column was equilibrated by flowing 0.01 M $CaCl_2{\cdot}2H_2O$ solutions (flow rate of 5 cm^3 min^{-1}) through the adsorbent for overnight (12 h) before the date of the actual experiments. The calcium chloride solution was used as the solvent phase to maintain a constant ionic strength and minimize cation exchange [17]. Besides, it can make the packing more compacted. Bromide ion, typically from potassium bromide (KBr) salts, is an inorganic conservative tracer, was chosen to trace the water flux through the column. Br^- breakthrough curves in each medium type presented in Fig. 2. As can be seen from Fig. 2 the column performance was well arranged for the actual experiments since typical *S*-shape curves were obtained in all column systems. Furthermore, VPum established more pronounced tailing, indicating that diffusional processes are operating. These Br^- breakthrough curves may be used to predict how the transport of any other compound is influenced by the hydraulic properties of the media.

Continuous up-flow column systems were set up, treating a continuous input of simulated water contaminated by a mixture of Cd(II) and Ni(II). The influent solution was pumped through the packed column with a peristaltic pump (MS-REGLO, Labortechnik-Analytik, Switzerland). The flow rates were routinely checked. The influent feed flow rate was varied and maintained throughout the experiments by use of the pump. At the exit of the column, the flow rate was measured to get steady-state flow conditions in the column. The effluent solution was collected at different time intervals using an automatic fraction collector (RFI, MA-RON GmbH, Germany). ICP-AES (inductively coupled plasma-atomic emission spectrometer, JY 238, Jobin Yvon, Longjumeau, France) was used to determine residual heavy metals (Cd(II) and Ni(II)) and eluted metal (Ca, Mg, Al, Fe, Na, and K) ion concentrations from the adsorbents in the solution. Because the influent was soluble at the target pH values (pH = 5 ± 0.1), head loss changes across the bed were not measured.

2.4. Analysis of breakthrough curve and design parameters

The time for breakthrough appearance and the shape of the breakthrough curve is very important features for determining an adsorption column's operation and dynamic response since they have a direct impact on the viability and economics of the adsorption processes [30]. The breakthrough curve profile and parameters are dependent on the operating conditions of the fixed-bed column such as influent flow rate, adsorbent particle size, influent heavy metals concentration, and media bed type (single and dual). To investigate the performance of the column and scale-up, the determination of such operating parameters through the experiment is very essential.

Breakthrough curves for adsorption of Cd(II) and Ni(II) on the adsorbents were obtained by plotting time against the ratio of concentrations of metal ions in the effluent and in the influent solutions C_{eff}/C_0. The breakthrough time (t_b) is usually defined as the time of adsorption when the effluent concentration (C_{eff}) from the column was about

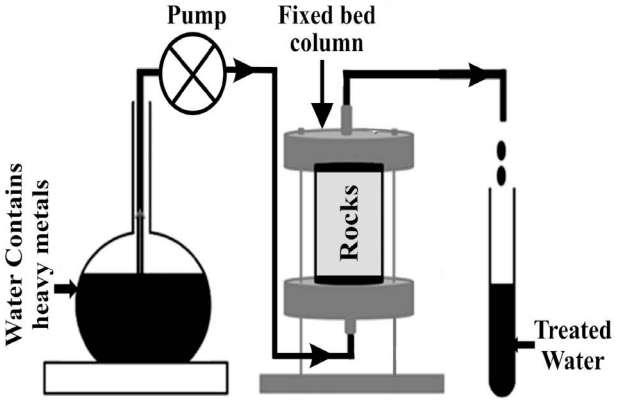

Fig. 1. Fixed bed column set-up.

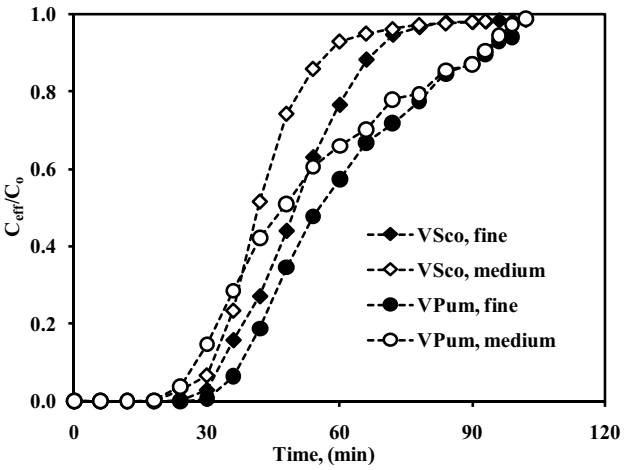

Fig. 2. Br^- breakthrough curves for different filter media type.

1% of the influent concentration (C_0) which represented the time that column was still active. Moreover, t_e (min) is exhaustion time, required to reach the exhaust point or $C_{eff}/C_0 = 0.99$.

In addition, the breakthrough volume of the treated water (V_{eff}, cm^3) was determined by multiplying the breakthrough time (t_b) with the volumetric flow rate (Q). Sorbent usage dose can also be determined at this point by dividing the sorbent mass (m_{ads}, g) in the column with the breakthrough water volume (V_{eff}) which represented the adsorbent exhaustion rate (Ads_R, g cm^{-3}). To estimate the efficiency of the sorption column, the retardation factor (r_f) is often employed to determine the rate at which the contaminants move faster in the column. Indeed r_f is determined from the breakthrough water volume (V_{eff}) per void volume (V_v).

Furthermore unused bed length (H_{UNB}) or mass transfer zone (MTZ) [31] can be obtained from Eq. (1).

$$H_{UNB} = MTZ = H_T\left(\frac{t_e - t_b}{t_e}\right) \tag{1}$$

where H_T is total bed height (cm), t_e (min) is exhaustion time, and t_b is breakthrough time (min).

The used bed length, H_B (cm) (up to the breakpoint) can also be obtained from Eq. (2).

$$H_B = \left(\frac{t_b}{t_e}\right)H_T \tag{2}$$

The empty bed contact time (EBCT) is one of the parameters frequently employed to examine the time required for a liquid to fill the empty column, can be obtained from Eq. (3).

$$EBCT = \frac{V_{bed}}{Q} \tag{3}$$

where V_{bed} is the volume of a fixed bed (cm^3) and Q is the flow rate ($cm^3\,min^{-1}$).

In addition, the total quantity of adsorbed heavy metal in the column was determined by mass conservation principle [32], from Eq. (4).

$$q = \frac{C_0V_0 - Q\int_0^t C_{eff}(t)dt - C_0V_v}{m_{ads}} \tag{4}$$

where q represents the mass of metal up taken onto the adsorbent (mg kg^{-1}), C_0 is the initial concentration of metal (mg cm^{-3}), V_0 is the total volume of water fed into column (cm^3), C_{eff} is the effluent concentration as a function of time (mg cm^{-3}), V_v is the void volume (cm^3), H_T is the bed height (cm), and t is the total time that column was operated (min).

2.5. Statistical analysis – Box–Behnken design

Based on the literature review, many studies on the fixed-bed column process were carried out by varying one factor while keeping all other factors fixed at a specific set of conditions [30–32]. This method was time-consuming and incapable of effective optimization. Recently, RSM has been employed to optimize and understand the performance of complex systems [33,34]. RSM is a type of mathematical and statistical technique used for experimental design, building models, assessing the relative significance of several independent variables synergism and determining the optimum conditions for a desirable response. By application of RSM, it was possible to evaluate the interactions of possible influencing factors on adsorption efficiency with a limited number of planned experiments [35]. In the present study, Box–Behnken design (BBD) was selected as standard RSM for optimizing the operating parameters (influent flow rate, initial heavy metal concentration, and particle size). The BBD was selected in this study because of its efficiency with respect to three-level designs that have various geometric constructions [36–38]. The Design Expert (Version 11) was used for data processing. Each independent variable was coded at 3 levels between –1 to +1, where the variables flow rate (A), initial heavy metal concentration (B) and particle size (C) were changed in the range of 2.50–5 mL min^{-1}, 2–50 mg L^{-1} and 0.075–2 mm, respectively. The variables and levels of the design model are given in Table S1.

In many engineering fields [33], it is common that the output variable (Y) exists with a set of predicted variables or the input variables (X_1, X_2, X_3, … X_k). The output variable is a function of input variables together with the error present in the model, usually written as $Y = f(X_1, X_2, X_3, \ldots X_k) + \in$, where f is the unknown surface response which is normally described by a first-order or second-order polynomial, while $\in$ is the error in the model. The first- and second-order models are given as in Eqs. (5) and (6), respectively:

$$Y = \beta_0 + \sum_{j=1}^{k}\beta_j X_j + \in \tag{5}$$

$$Y = \beta_0 + \sum_{j=1}^{k}\beta_j X_j + \sum_{j=1}^{k}\beta_{jj} X_j^2 + \sum_{j=1}^{k-1}\sum_{j=2}^{k}\beta_{ji} X_j X_i + \in_i \tag{6}$$

where Y is the output variable, X_i and X_j are coded independence variables and β_j, β_{jj} and β_{ji} (i = 1, 2, …, k; j = 1, 2 , …, k) are the regression coefficients. The second-order model describes a curving surface, including all terms in the first-order model, plus all quadratic terms like $\beta_{jj}X_j^2$, and all interaction terms like $\beta_{jj}X_jX_i$. The second-order model is also called the quadratic model. This model is generally adequate for RSM in most cases [33–35]. Experimental data were fitted to a second-order polynomial equation, and regression coefficients were obtained. The analysis of variance (ANOVA) was performed to justify the significance and adequacy of the developed regression model. The response surface model adequacy was evaluated by calculation of the determination coefficient (R^2) and testing it for the lack of fit. The main aim of the optimization was to maximize the adsorption capacity of Cd(II) and Ni(II) within the range of flow rate (A), initial heavy metal concentration (B) and particle size (C) for the treatment of simulated water by fixed-bed column adsorption process. The total number of experiments with three factors was seventeen. Twelve experiments were augmented with five replications at the design center to evaluate the pure error and were carried out in a randomized order as required in many design procedures. The number of the run, experimental conditions, the response of Cd(II) and Ni(II) adsorption capacity with the predicted values are given in Table 2.

3. Results and discussion

3.1. Effect of flow rate

To investigate the influence of flow rate through the column on removal efficiency, studies were conducted at different values of flow rates its varied from 2.5 to 5 mL min^{-1}, while the particle size of adsorbent and inlet heavy metal concentration was kept constant at 0.0425–2.0 mm and 2 mg L^{-1}, respectively. Fig. 3 (VPum) and Fig. 4 (VSco) show that the flow rate increases, the breakthrough curve becomes steeper while the breakthrough time decreased. The probable reason for the increase in the steepness of the breakthrough curve with an increase in the flow rate is that, when the residence time of heavy metal in the column is not long enough for adsorption stability to be reached at that flow rate, the heavy metal solution leaves the column before equilibrium occurs. This behavior may also be due to the insufficient residence time of heavy metal in the column and diffusion limitations of the metal into the pores of the rock [39].

As can be seen from Table 3, the value of the retardation factor was found to decrease with an increase in flow rate for both column systems, confirming that faster saturation of the adsorbent bed at a high flow rate. The reason for the faster saturation of the adsorbent bed at higher flow rates could be that with an increase in the flow rate, mixing increases, and the thickness of the liquid film surrounding the adsorbent particle decreases, thus reducing the film transfer resistance and an increase in the mass transfer rate. This was further verified by MTZ or unused bed (H_{UNB}) which decreased with decreasing flow rate (Table 3). In addition to that, the number of heavy metals adsorbed onto the adsorbent decreased with increasing flow rate, further indicating that at higher flow velocities, the film surrounding the particle breaks thereby reducing the adhesion of heavy metal to sorbent particle. A similar type of observation was reported by various authors for fixed-bed column systems [21,23,30,31].

Table 2
Experimental design matrix and response based on the experimental runs and predicted values on the Cd(II) and Ni(II) adsorption capacity as proposed by the BBD

Run	Flow rate, mL min^{-1}	Initial heavy metal concentration, mg L^{-1}	Particle size, mm	Cd(II) adsorption capacity, mg kg^{-1}		Ni(II) adsorption capacity, mg kg^{-1}	
				Actual	Predicted	Actual	Predicted
1	2.5	2	1.0375	28.64	28.49	36.86	38.01
2	5	2	1.0375	20.97	23.79	28.78	29.30
3	2.5	50	1.0375	44.25	41.43	42.3	41.78
4	5	50	1.0375	35.8	33.54	39.8	38.65
5	2.5	26	0.075	41.45	41.48	43.4	42.50
6	5	26	0.075	34.5	33.97	37.25	36.97
7	2.5	26	2	35.45	35.98	34.46	34.73
8	5	26	2	28.52	28.49	27.53	28.43
9	3.75	2	0.075	26.50	24.2	29.49	29.24
10	3.75	50	0.075	31.52	34.31	34.12	35.54
11	3.75	2	2	21.46	18.67	22.25	20.83
12	3.75	50	2	26.56	24.21	27.4	27.65
13	3.75	26	1.0375	33.50	33.50	32.50	32.50
14	3.75	26	1.0375	33.50	33.50	32.50	32.50
15	3.75	26	1.0375	33.50	33.50	32.50	32.50
16	3.75	26	1.0375	33.50	33.50	32.50	32.50
17	3.75	26	1.0375	33.50	33.50	32.50	32.50

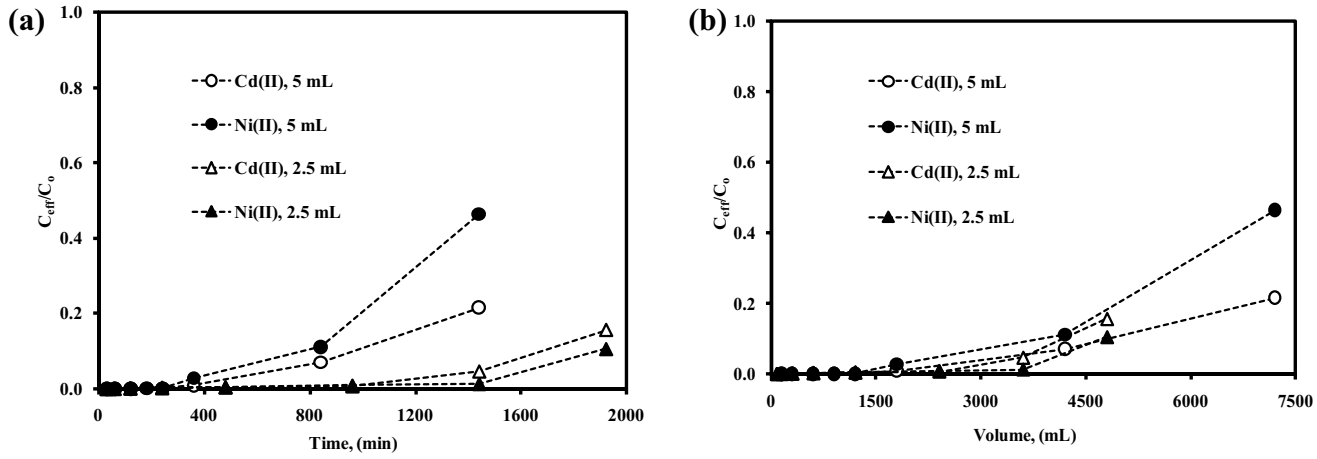

Fig. 3. Effect of flow rate on breakthrough curves for adsorption of Cd(II) and Ni(II) on VPum (a) C_{eff}/C_0 vs. time and (b) C_{eff}/C_0 vs. effluent volume.

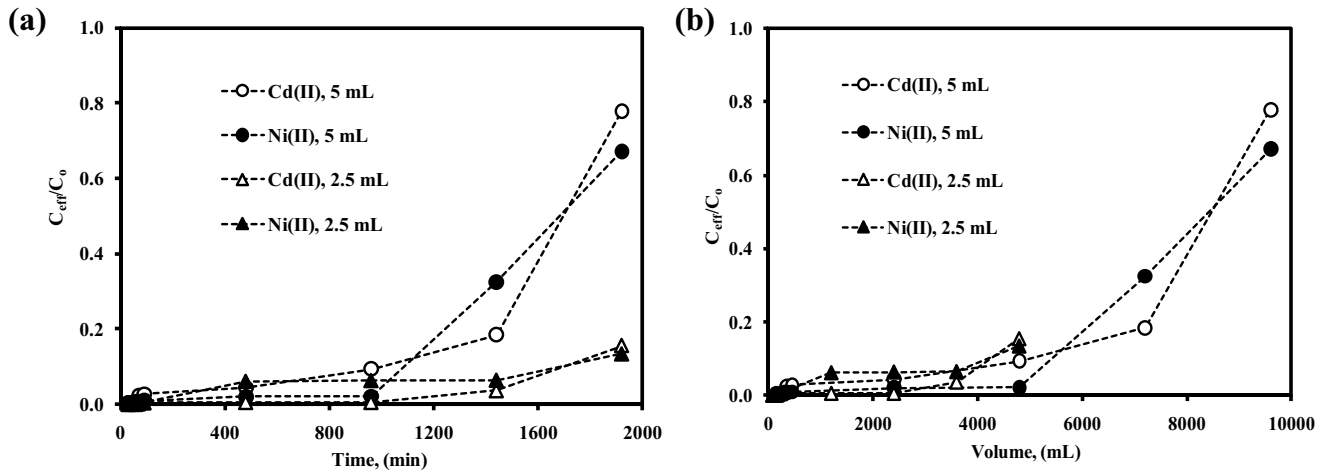

Fig. 4. Effect of flow rate on breakthrough curves for adsorption of Cd(II) and Ni(II) on VSco (a) C_{eff}/C_0 vs. time and (b) C_{eff}/C_0 vs. effluent volume.

3.2. Effect of initial concentration

The adsorption performance of VPum and VSco was tested by varying the inlet heavy metal concentration from 2 to 50 mg L^{-1}. The flow rate and particle size were kept constant at 5 mL min^{-1} and 0.425–2.0 mm, respectively. The effect of initial concentration on the performance of the breakthrough curve is shown in Fig. 5. A change in the initial heavy metal concentration has a significant influence on the characteristics of the breakthrough curve. At a relatively higher initial concentration of the heavy metals, the curves were steeper for both the effluents showing the faster exhaustion of the bed since binding sites become more quickly field in the system (Fig. 5). This can also be explained by the fact that at high initial concentration, a breakthrough occurred fast and the treated volume was smaller since the higher concentration gradient caused a faster transport due to increased diffusion coefficient or mass transfer coefficient was reported by Aksu and Ferda in 2004 as summarized by Sarin et al. [21].

In addition, as can be seen in Table 4 by changing the initial concentration of the solution from 2.0 to 50 mg L^{-1}, the absolute amount of adsorbed Cd(II) and Ni(II) was increased. This finding is well in agreement with the previous findings obtained from the batch experiments, the more concentrated the solution the better the uptake [14,15,40,41]. The initial heavy metal ion concentration acts as the driving force to overcome the mass-transfer barrier between the adsorbent and adsorbate medium.

3.3. Effect of particle size

The particle size of adsorbent is also an important parameter for the design of an adsorption column. Studies were conducted using two different particle sizes of VPum varied from 0.075–0.425 mm to 0.425–2.0 mm while the flow rate and the inlet heavy metal concentration were kept constant at 5 mL min^{-1} and 50 mg L^{-1}, respectively. The effect of particle size of adsorbent on the breakthrough

Table 3
Breakthrough analysis: effect of flow rate, VPum and VSco

Parameters	VPum			
	Q = 5 mL min^{-1}		Q = 2.5 mL min^{-1}	
	Cd(II)	Ni(II)	Cd(II)	Ni(II)
C_0 (mg L^{-1})	2	2	2	2
Size (mm)	0.0425–2.0	0.0425–2.0	0.0425–2.0	0.0425–2.0
V_{bed} (cm^3)	489.54	489.54	489.54	489.54
t_e (min)	1,440	1,440	1,920	1,920
t_b (min)	360	300	960	1,200
EBCT (min)	97.91	97.91	195.81	195.81
MTZ (cm)	7.13	7.52	4.75	3.56
H_B (cm)	2.37	1.98	4.75	3.56
V_{eff} (cm^3)	1,800	1,500	2,400	3,000
Ads_R (g cm^{-3})	0.13	0.15	0.10	0.08
r_f	4.61	3.84	6.15	7.68
q (mg kg^{-1})	25.972	32.778	28.64	36.86
Parameters	VSco			
	Q = 5 mL min^{-1}		Q = 2.5 mL min^{-1}	
	Cd(II)	Ni(II)	Cd(II)	Ni(II)
C_0 (mg L^{-1})	2	2	2	2
Size (mm)	0.0425–2.0	0.0425–2.0	0.0425–2.0	0.0425–2.0
V_{bed} (cm^3)	489.54	489.54	489.54	489.54
t_e (min)	960	960	1,920	1,920
t_b (min)	69	120	285	480
EBCT (min)	97.91	97.91	195.81	195.81
MTZ (cm)	9.16	8.91	8.09	7.13
H_B (cm)	0.34	0.59	1.41	2.37
V_{eff} (cm^3)	345	600	712.5	1,200
Ads_R (g cm^{-3})	1.76	1.01	0.85	0.51
r_f	1.22	2.11	2.51	4.23
q (mg kg^{-1})	7.7	11.9	10.2	12.5

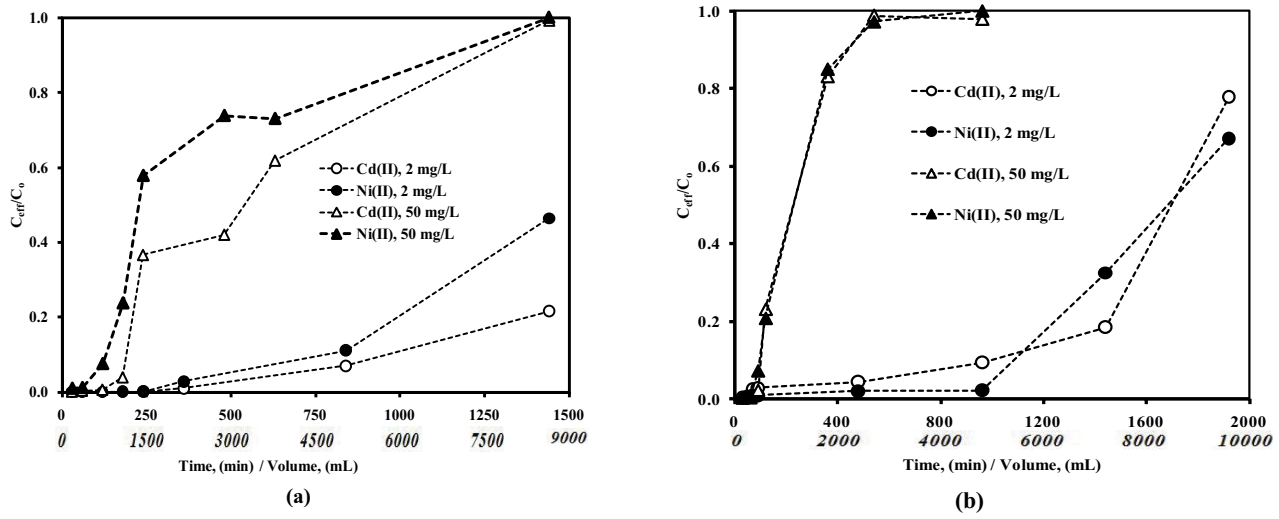

Fig. 5. Effect of initial concentration on breakthrough curves for adsorption of Cd(II) and Ni(II) on (a) VPum and (b) VSco.

Table 4
Breakthrough analysis: effect of initial concentration, VPum and VSco

	VPum			
	C_0 = 50 mg L^{-1}		C_0 = 2 mg L^{-1}	
Parameters	Cd(II)	Ni(II)	Cd(II)	Ni(II)
t_b (min)	120	60	360	300
V_{eff} (cm^3)	600	300	1,800	1,500
Ads_R (g cm^{-3})	0.38	0.769	0.13	0.15
r_f	1.54	0.768	4.61	3.84
q (mg kg^{-1})	43.8	22.84	25.972	32.778
	VSco			
t_b (min)	65	90	69	120
V_{eff} (cm^3)	325	450	345	600
V_{eff} (cm^3)	325	450	345	600
r_f	1.15	1.59	1.22	2.11
q (mg kg^{-1})	7.2	39.3	7.7	11.9

curve is shown in Fig. 6. The parameters for the column study such as breakthrough time, retardation factor, breakthrough sample volume, and adsorbent exhaustion rate obtained from the breakthrough analysis are summarized in Table 5.

As can be seen from the breakthrough curves, a higher breakpoint time of the process was achieved at smaller particle sizes. As the particle size of adsorbent increases, breakthrough time was obtained earlier. Moreover, the breakthrough volume decreased from 0.6 to 0.3 L for Cd(II) removal and from 0.3 to 0.15 L for Ni(II) removal, respectively as the particle size was increased from fine to medium size. As it is also evident from Fig. 6, for bigger adsorbent size, the rate of adsorbent exhaustion was higher which shows faster exhaustion of fixed bed. In addition, by changing the adsorbent particle size from medium to fine, the total quantity of adsorbed heavy metals was increased (Table 5). This can be explained by the fact that at smaller adsorbent particle size, surface areas for sorption becomes large, and hence, the higher removal efficiency was obtained. The effect of particle sizes in the case of VPum was demonstrated in column experiments than that of previously conducted batch experiments [17,18], indicating that its adsorption capacity depends on the size of the particles.

3.4. Effect of media bed type

The effectiveness of different adsorbents media beds such as single media bed: VSco; dual media bed: containing both VPum and VSco in Cd(II) and Ni(II) removal efficiency was evaluated. The adsorbents were packed into columns in a stepwise procedure. First, 4.25 cm of VSco was transferred into the column and was shaken manually in order to have dense packing. Next, an equal amount (4.25 cm layer) of VPum at the top of the VSco transferred. The flow rate, the particle size of the adsorbent, and the inlet heavy metal concentration were kept constant at 2.5 mL min^{-1}, 0.0425–2.0 mm, and 2 mg L^{-1}, respectively. The effect of media bed type on the breakthrough curve is shown in Fig. 7.

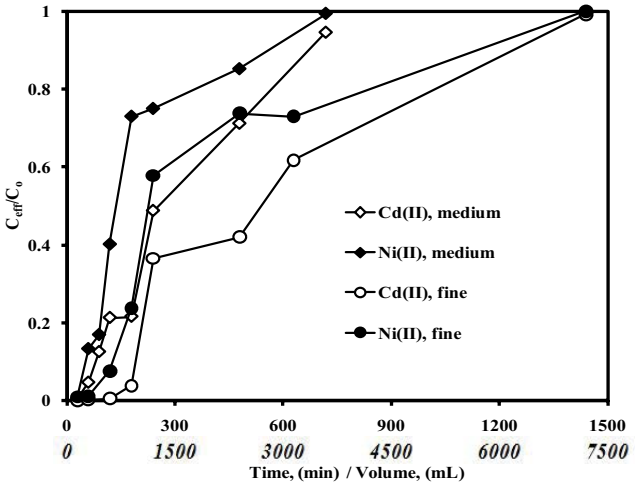

Fig. 6. Effect of particle size on breakthrough curves for adsorption of Cd(II) and Ni(II) on VPum.

Table 5
Breakthrough analysis: effect of adsorbent particle size

	VPum, medium		VPum, fine	
Parameters	Cd(II)	Ni(II)	Cd(II)	Ni(II)
t_b (min)	60	30	120	60
t_e (min)	≈720	720	1,440	≈1,440
V_{eff} (cm^3)	300	150	600	300
Ads_R (g cm^{-3})	0.49	0.98	0.38	0.769
r_f	0.72	0.36	1.54	0.768
q (mg kg^{-1})	11.2	142.3	43.8	228.4

As can be seen from the breakthrough curves, a higher breakpoint time of the process was achieved at dual media bed type (Fig. 7). As the media bed type single, breakthrough time was obtained earlier. The parameters for the column study such as breakthrough time, breakthrough volume, adsorbent exhaustion rate, retardation factor, and absolute amount of adsorbed Cd(II) and Ni(II) obtained from the breakthrough analysis are summarized in Table 6. For a single bed type, the rate of adsorbent exhaustion was higher which shows faster exhaustion of fixed bed (Table 6).

In addition, as can be seen from Table 6 dual media column containing VSco and VPum reduced Cd(II) and NI(II) concentration appreciably, and were found more than the single column containing VSco. This can be explained by the fact that by applying the dual media, binding sites for sorption becomes large, and hence, heavy metal had more time to contact with the adsorbent that resulted in higher removal efficiency, which might be important for technical consideration when VSco is used for water purification purposes. However, in order to reach the final conclusion longtime breakthrough analysis must be conducted.

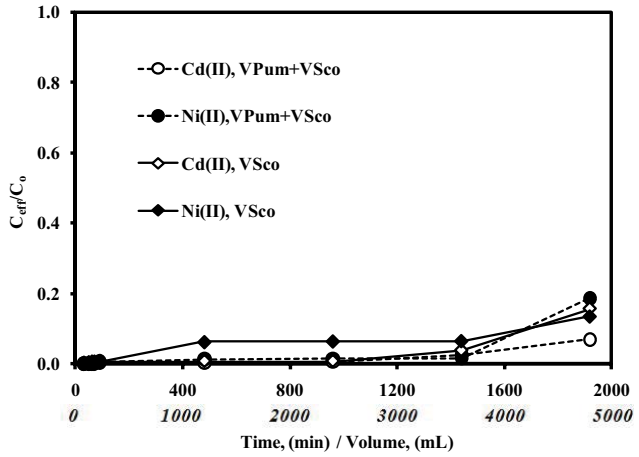

Fig. 7. Effect of media bed type on breakthrough curves for adsorption of Cd(II) and Ni(II) on dual and single bed media.

Table 6
Breakthrough analysis: effect of media bed type

	VSco, fine		Dual media (VSco + VPum)	
Parameters	Cd(II)	Ni(II)	Cd(II)	Ni(II)
t_b (min)	285	480	1,200	960
V_{eff} (cm^3)	712.5	1,200	3,000	2,400
Ads_R (g cm^{-3})	0.85	0.51	0.14	0.17
r_f	2.51	4.23	8.90	7.12
q (mg kg^{-1})	10.2	12.5	16.2	19.6

3.5. Sorption mechanism investigation

The elution of Ca, Mg, Na, K, Al, and Fe ions from the adsorbent during the treatment process was investigated. Insignificant quantities of the cations were detected in treated water (data not shown). It is, therefore, suggested that ion-exchange is not the main mechanism involved in the uptake of heavy metal by the adsorbents. Thus, the heavy metals sorption is due to the electrostatic phenomenon as well as surface complexation that work individually or in combinations for the adsorption of Cd(II) and Ni(II) ions on the adsorbents. These conclusions are in agreement with the batch experiments findings of previous studies [17,18].

In addition, the variation in pH with elution was also recorded and the results presented in the supplementary material (Fig. S2). In most cases, effluent pH sharply increased to pH 7.4–7.7 within 600 mL effluent volume, which is due to an acid neutralization effect and proton adsorption of hydroxylated rock surface. Similar observations were also reported in the previous batch experiments [17,18]. And then the final pH values (pHfin) dropped to pH 5.8–6.1 within ≥1,200 mL effluent volumes due to the sorbent protonation effect. This finding further confirms that both surface complexation and electrostatic attraction as well as diffusion into micropores of the adsorbent are mainly responsible for the immobilization of Cd(II) and Ni(II) in the presence of volcanic material.

Furthermore, the removal capacity of the rocks obtained from batch systems with the column systems was compared. By comparison of the results obtained from this study to the previously reported batch experiments for Cd(II) and Ni(II) ions, in most cases, it can be stated that relatively higher adsorption capacities were observed in batch operation compared to in fixed-bed column. The experimental results showed that the removal capacity from batch experiments under mixture matrices was 21.8 mg Cd(II) kg^{-1} and 20.2 mg Ni(II) kg^{-1} of VSco and 30.2 mg Cd(II) kg^{-1} and 28 mg Ni(II) kg^{-1} of VPum [17,18], which was not comparable to columns data of 7.7 mg Cd(II) kg^{-1} and 11.9 mg Ni(II) kg^{-1} of VSco and 26 mg Cd(II) kg^{-1} and 33 mg Ni(II) kg^{-1} of VPum obtained from column study (Table 4). This difference was not explained by reaction kinetics alone. We believe it is mainly due to preferential flows in column experiments, favoring metal ion elution. In view of the results presented here, more research is needed to predict the column design.

3.6. Evaluation of experimental results with the design of experiments: adequacy of the model tested

Three factors and 3 levels BBD was applied to optimize the mutual effects of the independent variables such as flow rate (A), initial heavy metal concentration (B) and particle size (C) on the adsorption Cd(II) (Y_1) and Ni(II) (Y_2) onto volcanic rocks. The design of the experiment and the results of the RSM tests are listed in Table 2. According to the results of RSM, a second-order polynomial regression equation for describing the adsorption capacity of Cd(II) and Ni(II) can be expressed as follows:

$$\text{Cd(II) adsorption capacity (mg kg}^{-1}) \; Y_1 = 33.50 - 3.75A + 5.07B - 2.75C - 0.1950AB + 0.0050AC + 0.0200BC + 3.69A^2 - 4.78B^2 - 2.21C^2 \quad (7)$$

$$\text{Ni(II) adsorption capacity (mg kg}^{-1}) \; Y_2 = 32.50 - 2.96A + 3.28B - 4.08C + 1.39AB - 0.1950AC + 0.1300BC + 5.89A^2 - 1.46B^2 - 2.73C^2 \quad (8)$$

Experimental data were analyzed by two different tests, namely the sequential model sum of squares and model summary statistics in order to obtain effective regression models among various models such as linear, interactive, quadratic, and cubic. The results are tabulated in the supplementary Tables S2 and S3 for the Cd(II) adsorption and Ni(II) adsorption, respectively. It can be seen from the Tables S2 and S3, the cubic model was found to be aliased, which cannot be used for further modeling of experimental data [33]. For quadratic and linear models, p-values were lower than 0.004, and both of these models could be used for further study as per sequential model of the sum of squares test. However, the model summary statistics showed that after excluding the cubic model which was aliased, the quadratic model was found to have the maximum "adjusted R" and "Predicted R" values. Therefore, the quadratic model was chosen for further analysis. The goodness of fit by the quadratic equation was verified by the determination of the

regression coefficient (R^2). The value of R^2 for the quadratic equations was 0.912 (Table S2) and 0.981 (Table S3) for Cd(II) and Ni(II) adsorption, respectively, which indicate that prediction of the adsorption efficiency by the polynomial model was excellent. The comparison between the experimental and predicted value from the model is also indicated in the supplementary materials (Figs. S3a and b). It was observed that the model predictions matched the experimental values and the data points lay close to the diagonal line.

Furthermore, ANOVA was carried out to justify the significance and adequacy of the regression model and the results are summarized in Tables 7 and 8. It could be seen from Tables 7 and 8 for the Cd(II) and Ni(II) adsorption efficiency, the linear coefficients of flow rate (*A*), initial heavy metals concentration (*B*), and particle size (*C*), and the interaction effect of flow rate (*A*) × initial metal concentration (*B*), flow rate (*A*) × particle size (*C*), initial heavy metal concentration (*B*) × particle size (C) as well as the quadratic coefficient of flow rate (A^2), initial heavy metal concentration (B^2), and particle size (C^2) are significant factors at a level less than 5%. Thus, the ANOVA analysis confirms that the form of the model chosen to explain the relationship between the factors and the response is correct.

Adequacy check is crucial to make sure the approximation model can give an adequate approximation to prevent poor and misleading results [34]. In the present study, "Adeq Precision" that measures the signal-to-noise ratio was computed. The result for Cd(II) and Ni(II) adsorption capacity was found to be 10.83 and 24.76, respectively, which indicated there was an adequate signal. Hence, the second-order model can be used to navigate the design space.

3.7. Combined effect of operating parameters for Cd(II) and Ni(II) adsorption capacity

The effect of operating parameters obtained from the response surface analysis to estimate the maximum Cd(II) and Ni(II) adsorption capacity with respect to each variable and the effects of each variable on the Cd(II) and Ni(II) adsorption capacity is discussed in the following subsections.

3.7.1. Effect of flow rate (A) with initial heavy metal concentration (B)

The combined effect of flow rate (*A*) and initial heavy metal concentration (*B*) on Cd(II) and Ni(II) adsorption capacity was carried out by varying A from 2.5 to 5 mL min^{-1} under different *B* from 2 to 50 mg L^{-1}. The results are given in Table 2 and plotted in Figs. 8a and b. From Figs. 8a and b, the Cd(II) and Ni(II) adsorption capacity were decreased with an increase in flow rate at any value of initial heavy metal concentration. The probable reason for the increase in the flow rate is that, when the residence time of heavy metal in the column is not long enough for the adsorption stability to be reached at that flow rate, the heavy metal solution leaves the column before equilibrium occurs. This behavior may also be due to insufficient residence time of heavy metal in the column and the diffusion limitations of the metal into the pores of the rock. Similarly, the combined effect of flow rate (*A*) and particle size (*C*) on Cd(II) and Ni(II) adsorption capacity was carried out by varying *A* from 2.5 to 5 mL min^{-1} under different *C* from 0.075 to 2 cm. the results are given in Supplementary Fig. S4. The Cd(II) and Ni(II) adsorption capacity were increased with decreasing particle size (*C*) at any value flow rate (*A*).

3.7.2. Effect of initial heavy metal concentration (B) with particle size (C)

The effect of initial heavy metal concentration (*B*) and particle size (*C*) for the better Cd(II) and Ni(II) adsorption capacity was evaluated. The effects of particle size (*C*) and initial heavy metal concentration (*B*) on Cd(II) and Ni(II) adsorption capacity under different *C* (from 0.075 to 2 cm) and *B* (from 2 to 50 mg L^{-1}) are plotted in Fig. 9a and b. It was observed that the Cd(II) and Ni(II) adsorption capacity was decreased with increasing particle size from 0.075 to 2 mm

Table 7
ANOVA for a quadratic model for Cd(II) adsorption capacity

Source	Sum of squares	df	Mean square	*F*-value	*p*-value	
Model	546.66	9	60.74	8.06	0.0059	Significant
A-Flow rate	112.50	1	112.50	14.93	0.0062	Significant
B-Initial metal concentration	205.64	1	205.64	27.30	0.0012	Significant
C-Particle size	60.39	1	60.39	8.02	0.0254	Significant
AB	0.1521	1	0.1521	0.0202	0.8910	
AC	0.0001	1	0.0001	0.0000	0.9972	
BC	0.0016	1	0.0016	0.0002	0.9888	
A^2	57.41	1	57.41	7.62	0.0281	Significant
B^2	96.10	1	96.10	12.76	0.0091	Significant
C^2	20.61	1	20.61	2.74	0.1421	
Residual	52.73	7	7.53			
Lack of fit	52.73	3	17.58			
Pure error	0.0000	4	0.0000			
Corr. total	599.39	16				

Table 8
ANOVA for a quadratic model for Ni(II) adsorption capacity

Source	Sum of squares	df	Mean square	*F*-value	*p*-value	
Model	474.79	9	52.75	40.49	<0.0001	Significant
A-Flow rate	69.97	1	69.97	53.71	0.0002	Significant
B-Initial metal concentration	86.07	1	86.07	66.06	<0.0001	Significant
C-Particle size	133.01	1	133.01	102.09	<0.0001	Significant
AB	7.78	1	7.78	5.97	0.0445	Significant
AC	0.1521	1	0.1521	0.1167	0.7426	
BC	0.0676	1	0.0676	0.0519	0.8263	
A^2	146.07	1	146.07	112.11	<0.0001	Significant
B^2	8.91	1	8.91	6.84	0.0346	Significant
C^2	31.38	1	31.38	24.09	0.0017	Significant
Residual	9.12	7	1.30			
Lack of fit	9.12	3	3.04			
Pure error	0.0000	4	0.0000			
Corr. total	483.91	16				

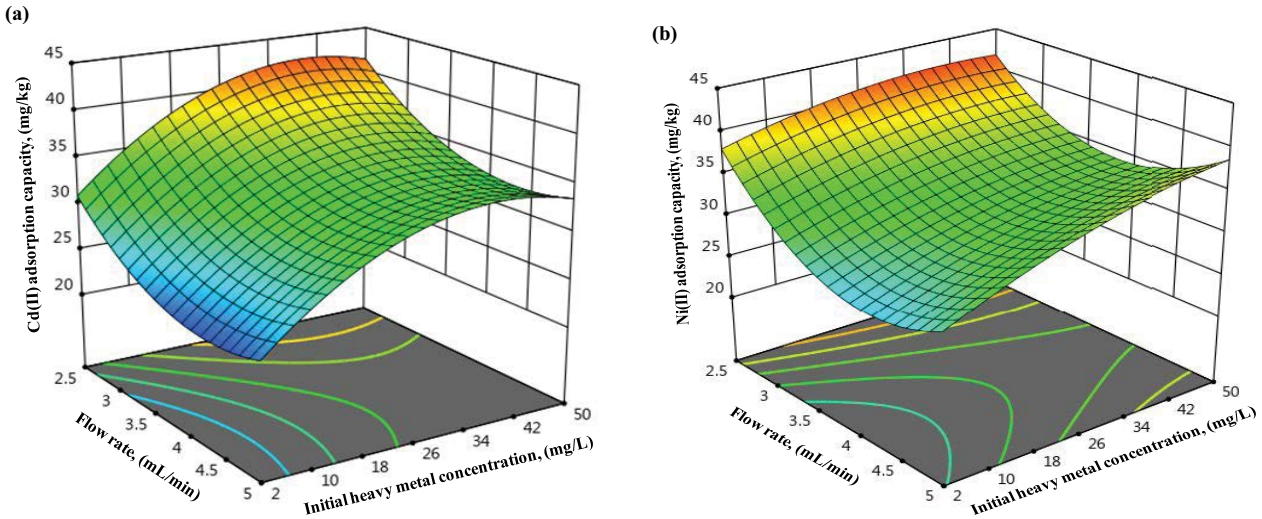

Fig. 8. Combined effect of flow rate (a) and initial heavy metal concentration (b) on (a) Cd(II) and (b) Ni(II) adsorption capacity.

at any value of initial heavy metal concentration. This can be explained by the fact that at the smaller adsorbent particle size, surface areas for sorption becomes large, and hence, higher removal efficiency obtained.

In order to achieve the maximum adsorption of Cd(II) and Ni(II) onto VSco and VPum the optimum conditions were about flow rate (*A*) – 2.50 mL min^{-1}, initial heavy metal concentration (*B*) – 39.50 mg L^{-1} and particle size (*C*) – 0.40 mm, with the yield of Cd(II) adsorption of 40.75%, and Ni(II) adsorption of 43.25% with the influent pH of 5. A mean value of 40.25% and 42.75% for Cd(II) and Ni(II) adsorption capacity were obtained from the experimental, which is in close agreement with the predicted values obtained (Table 2). The good correlation between these actual and predicted results indicates that the reliability of BBD incorporates the desirability function method and it could be effectively used to optimize the up-flow fixed-bed column adsorption process parameters for any type of wastewater and industrial effluent.

4. Conclusions

The results of this research have provided information about the suitability of VPum and VSco to adsorb Cd(II) and Ni(II) ions from water under flow conditions. Up-flow fixed-bed column adsorption studies have shown that Cd(II) and Ni(II) removal was a strong function of initial sorbent concentration, flow rate, and particle size. As these design parameters increased, the breakthrough curve became steeper and the breakpoint time shorter. For a VPum bed, the greater removal efficiency was observed in comparison to a VSco bed under the same experimental conditions. A dual-media column of VPum and VSco was found most economical and effective in removing of Cd(II) and Ni(II).

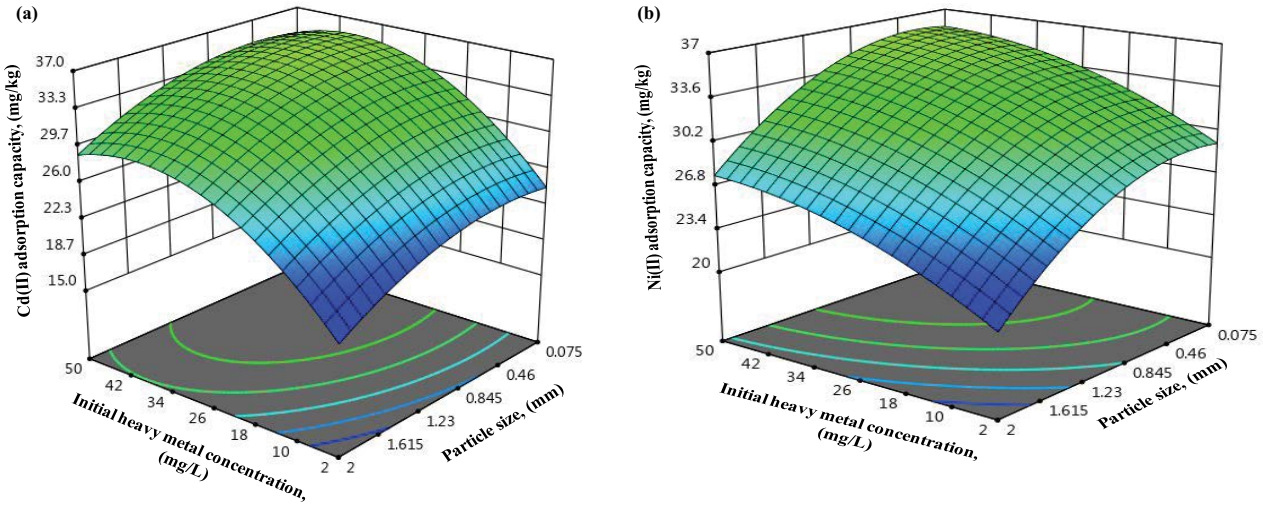

Fig. 9. Combined effect of initial heavy metal concentration and particle size on (a) Cd(II) and (b) Ni(II) adsorption capacity.

The RSM using BBD was successfully applied for experimental design, analysis of results, and optimization of the operating conditions for maximizing Cd(II) and Ni(II) removal. An analysis of regression equations obtained by Design Expert.11 showed a high coefficient of determination value (R^2 = 0.9120) for Cd(II) removal and (R^2 = 0.9812) for Ni(II) removal and thus ensuring a satisfactory fit of the second-order regression model with that of the experimental data. Further studies at the pilot-scale are also needed to examine the potential of the rocks.

References

[1] T. Alemayehu, Heavy metal concentration in the urban environment of Addis Ababa, Ethiopia, Soil Sediment Contam., 15 (2006) 591–602.
[2] P.N.M. Schipper, L.T.C. Bonten, A.C.C. Plette, S.W. Moolenaar, Measures to diminish leaching of heavy metals to surface waters from agricultural soils, Desalination, 226 (2008) 89–96.
[3] M. Kato, S. Onuma, Y. Kato, N.D. Thang, I. Yajima, M.Z. Hoque, H.U. Shekhar, Toxic elements in well water from Malaysia, Toxicol. Environ. Chem., 9 (2010) 1609–1612.
[4] J. Godt, F. Scheidig, C. Grosse-Siestrup, V. Esche, P. Brandenburg, A. Reich, D.A. Groneberg, The toxicity of cadmium and resulting hazards for human health, J. Occup. Med. Toxicol., 1 (2006) 22.
[5] WHO, Guidelines for Drinking Water Quality, First Addendum to 3rd ed., Vol. 1: Recommendations, World Health Organization, Geneva, Switzerland, 2006.
[6] W. Teeyakasem, M. Nishijo, R. Honda, S. Satarug, W. Swaddiwudhipong, W. Ruangyuttikarn, Monitoring of cadmium toxicity in a Thai population with high-level environmental exposure, Toxicol. Lett., 169 (2007) 185–195.
[7] Y. Mu, X.-J. Zheng, H.-Q. Yu, Determining optimum conditions for hydrogen production from glucose by an anaerobic culture using response surface methodology (RSM), Int. J. Hydrogen Energy, 34 (2009) 7959–7963.
[8] I. Mironyuk, T. Tatarchuk, Mu. Naushad, H. Vasylyeva, I. Mykytyn, Highly efficient adsorption of strontium ions by carbonated mesoporous TiO_2, J. Mol. Liq., 285 (2019) 742–753.
[9] Mu. Naushad, Z.A. ALOthman, Separation of toxic Pb^{2+} metal from aqueous solution using strongly acidic cation-exchange resin: analytical applications for the removal of metal ions from pharmaceutical formulation, Desal. Water Treat., 53 (2015) 2158–2166.
[10] M.M. Benjamin, R.S. Sletten, R.P. Bailey, T. Bennett, Sorption and filtration of metals using iron-oxide-coated sand, Water Res., 30 (1996) 2609–2620.
[11] F.L. Fu, Q. Wang, Removal of heavy metal ions from wastewaters: a review, J. Environ. Manage., 3 (2011) 407–418.
[12] S. Babel, T.A. Kurniawan, Low-cost adsorbents for heavy metals uptake from contaminated water: a review, J. Hazard. Mater., 97 (2003) 219–243.
[13] V.K. Gupta, P.J.M. Carrott, M.M.L. Ribeiro Carrott, Suhas, Low-cost adsorbents: growing approach to wastewater treatment—a review, Crit. Rev. Env. Sci. Technol., 39 (2009) 783–842.
[14] F. Melak, E. Alemayehu, A. Ambelu, E. Van Ranst, G. Du Laing, Evaluation of natural quartz and zeolitic tuffs for As(V) removal from aqueous solutions: a mechanistic approach, Int. J. Environ. Sci. Technol., 15 (2018) 217–230.
[15] S. Gupta, B.V. Babu, Modeling, simulation, and experimental validation for continuous Cr(VI) removal from aqueous solutions using sawdust as an adsorbent, Bioresour. Technol., 100 (2009) 5633–5640.
[16] S.S. Gupta, K.G. Bhattacharyya, Immobilization of Pb(II), Cd(II) and Ni(II) ions on kaolinite and montmorillonite surfaces from aqueous medium, J. Environ. Manage., 87 (2008) 46–58.
[17] E. Alemayehu, B. Lennartz, Virgin volcanic rocks: kinetics and equilibrium studies for the adsorption of cadmium from water, J. Hazard. Mater., 169 (2009) 395–401.
[18] E. Alemayehu, B. Lennartz, Adsorptive removal of nickel from water using volcanic rocks, Appl. Geochem., 25 (2010) 1596–1602.
[19] M.N. Sepehr, A. Amrane, K.A. Karimaian, M. Zarrabi, H.R. Ghaffari, Potential of waste pumice and surface modified pumice for hexavalent chromium removal: characterization, equilibrium, thermodynamic and kinetic study, J. Taiwan Inst. Chem. Eng., 45 (2014) 635–647.
[20] J.-S. Kwon, S.-T. Yun, J.-H. Lee, S.-O, Kim, H.Y. Jo, Removal of divalent heavy metals (Cd, Cu, Pb, and Zn) and arsenic(III) from aqueous solutions using scoria: kinetics and equilibria of sorption, J. Hazard. Mater., 174 (2010) 307–313.
[21] V. Sarin, T.S. Singh, K.K. Pant, Thermodaynamic and breakthrough column studies for the selective sorption of chromium from industrial effluent on activated eucalyptus bark, Bioresour. Technol., 97 (2006) 1986–1993.
[22] N.A.A. Nazri, R.S. Azis, H.C. Man, A.H. Shaari, N.M. Saiden, I. Ismail, Equilibrium studies and dynamic behavior of cadmium adsorption by magnetite nanoparticles extracted from mill scales waste, Desal. Water Treat., 171 (2019) 115–131
[23] S.H. Chen, Q.Y. Yue, B.Y. Gao, Q. Li, X. Xu, K.F. Fu., Adsorption of hexavalent chromium from aqueous solution by modified

corn stalk: a fixed-bed column study, Bioresour. Technol., 113 (2012) 114–120.
[24] H.A. Aziz, M.N. Adlan, K.S. Ariffin, Heavy metals (Cd, Pb, Zn, Ni, Cu and Cr(III)) removal from water in Malaysia: post treatment by high quality limestone, Bioresour. Technol., 99 (2008) 1578–1583.
[25] C. Reimann, K. Bjorvatn, B. Frengstad, Z. Melaku, R. Tekle-Haimanot, U. Siewers, Drinking water quality in the Ethiopian section of the East African Rift Valley I—data and health aspects, Sci. Total Environ., 311 (2003) 65–80.
[26] American Water Works Association, AWWA Standard for Filtering Material, ANSI/AWWA, American National Standard, 1998, pp. B100–96.
[27] R. Paramasivam, S.K. Gadkari, N.S. Joshi, A.W. Deshpande, Bituminous coal–a substitute for anthracite filter media in two layer filtration of water, Indian J. Environ. Health, 16 (1973) 178–188.
[28] B. Mörgeli, K.J. Ives, New media for effluent filtration, Water Res., 13 (1979) 1001–1007
[29] M.I. Al-Wakeel, Characterization and process development of the Nile diatomaceous sediment, Int. J. Miner. Process., 92 (2009) 128–136.
[30] I.-P. Chen, C.-C. Kan, C.M. Futalan, M.J.C. Calagui, S.-S. Lin, W.C. Tsai, M.-W. Wan, Batch and fixed bed studies: removal of copper(II) using chitosan-coated kaolinite beads from aqueous solution, Sustainable Environ. Res., 25 (2015) 73–81.
[31] M.T. Yagub, T.K. Sen, S. Afroze, H.M. Ang, Fixed-bed dynamic column adsorption study of methylene blue (MB) onto pine cone, Desal. Water Treat., 55 (2015) 1026–1039.
[32] R. Apiratikul, P. Pavasant, Batch and column studies of biosorption of heavy metals by *Caulerpa lentillifera*, Bioresour. Technol., 99 (2008) 2766–2777.
[33] P. Asaithambi, D. Beyene, A.A.A. Aziz, E. Alemayehu, Removal of pollutants with determination of power consumption from landfill leachate wastewater using an electrocoagulation process: optimization using response surface methodology (RSM), Appl. Water Sci., 69 (2018) 1–12.
[34] P. Asaithambi, E. Alemayehu, B. Sajjadi, A.R.A. Aziz, Electrical energy per order determination for the removal pollutant from industrial wastewater using UV/Fe^{2+}/H_2O_2 process: optimization by response surface methodology, Water Resour. Ind., 18 (2017) 17–32.
[35] R.H. Myers, D.C. Montgomery, C.M. Anderson-Cook, Response Surface Methodology: Process and Product Optimization Using Design Experiments, 2nd ed., John Wiley & Sons, USA, 2009.
[36] B.-y. Tak, B.-s. Tak, Y.-j. Kim, Y.-j. Park, Y.-h. Yoon, G.-h. Min, Optimization of color and COD removal from livestock wastewater by electrocoagulation process: application of Box–Behnken Design (BBD), J. Ind. Eng. Chem., 28 (2015) 307–315.
[37] J. Rumky, M.C. Ncibi, R.C. Burgos-Castillo, A. Deb, M. Sillanpää, Optimization of integrated ultrasonic-Fenton system for metal removal and dewatering of anaerobically digested sludge by Box-Behnken Design, Sci. Total Environ., 645 (2018) 573–584.
[38] L. Adlnasab, N. Shekari, A. Maghsodi, Optimization of arsenic removal with Fe_3O_4@Al_2O_3@Zn-Fe LDH as a new magnetic nano adsorbent using Box-Behnken design, J. Environ. Chem. Eng., 7 (2019) 102974.
[39] F. Gode, E. Moral, Column study on the adsorption of Cr(III) and Cr(VI) using Pumice, Yarikkaya brown coal, Chelex-100 and Lewatit MP 62, Bioresour. Technol., 99 (2008) 1981–1991.
[40] E. Alemayehu, S. Thiele-Bruhn, B. Lennartz, Adsorption behavior of Cr(VI) onto macro and micro-vesicular volcanic rocks from water, Sep. Purif. Technol., 78 (2011) 51–61.
[41] E. Alemayehu, F. Melak, S.K. Sharma, B. van der Bruggen, B. Lennartz, Use of porous volcanic rocks for the adsorptive removal of copper, Water Environ. J., 31 (2017) 194–201.

Supplementary information

Table S1
Coded and actual values of the variables of the design of experiments for up-flow fixed-bed column adsorption process

Variable	Unit	Factor	Levels		
			–1	0	+1
Flow rate	mL min^{-1}	*A*	2.50	3.75	5
Initial heavy metal concentration	mg L^{-1}	*B*	2	26	50
Particle size	mm	*C*	0.075	1.0375	2

Table S2
Sequential model sum of squares and model summary statistics for Cd(II) adsorption capacity

Sequential model sum of squares						
Source	Sum of squares	df	Mean square	*F*-value	*p*-value	
Mean vs. total	17,351.73	1	17,351.73			
Linear vs. mean	378.53	3	126.18	7.43	0.0048	
2FI vs. linear	0.1538	3	0.0513	0.0023	0.9998	
Quadratic vs. 2FI	167.98	3	55.99	7.43	0.0040	Suggested
Cubic vs. quadratic	52.73	3	17.58			Aliased
Residual	0.0000	4	0.0000			
Total	17,951.11	17	1,055.95			
Model summary statistics						
Source	Standard deviation	R^2	Adjusted R^2	Predicted R^2	PRESS	
Linear	4.12	0.6315	0.5465	0.2481	450.70	
2FI	4.70	0.6318	0.4109	–0.8113	1,085.67	
Quadratic	2.74	0.9120	0.8989	0.9076	843.68	Suggested
Cubic	0.0000	1.0000	1.0000			Aliased

Table S3
Sequential model sum of squares model summary statistics for Ni(II) adsorption capacity

Sequential model sum of squares						
Source	Sum of squares	df	Mean square	*F*-value	*p*-value	
Mean vs. total	18,853.79	1	18,853.79			
Linear vs. mean	289.05	3	96.35	6.43	0.0066	
2FI vs. linear	8.00	3	2.67	0.1428	0.9320	
Quadratic vs. 2FI	177.73	3	59.24	45.47	<0.0001	Suggested
Cubic vs. quadratic	9.12	3	3.04			Aliased
Residual	0.0000	4	0.0000			
Total	19,337.70	17	1,137.51			
Model summary statistics						
Source	Standard deviation	R^2	Adjusted R^2	Predicted R^2	PRESS	
Linear	3.87	0.5973	0.5044	0.1635	404.78	
2FI	4.32	0.6139	0.3822	–0.9572	947.10	
Quadratic	1.14	0.9812	0.9569	0.7984	145.92	Suggested
Cubic	0.0000	1.0000	1.0000			Aliased

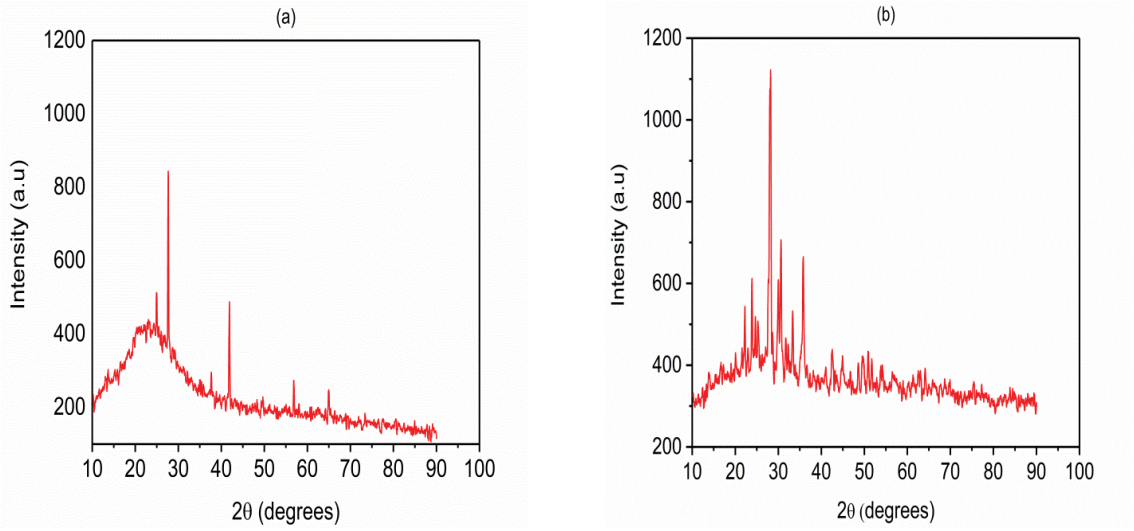

Fig. S1. XRD patterns for (a) VPum and (b) (VSco).

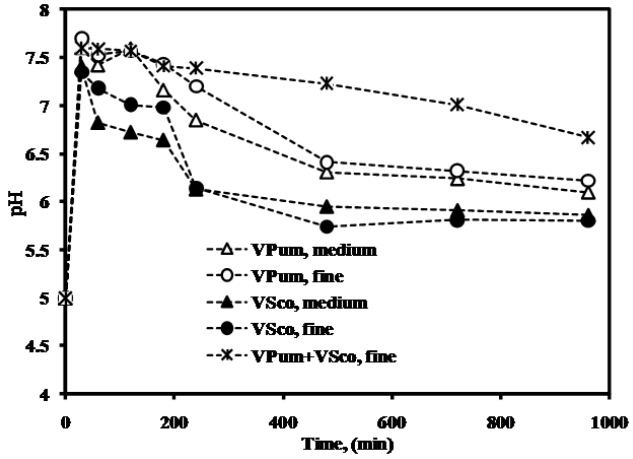

Fig. S2. pH variation in fixed bed column systems.

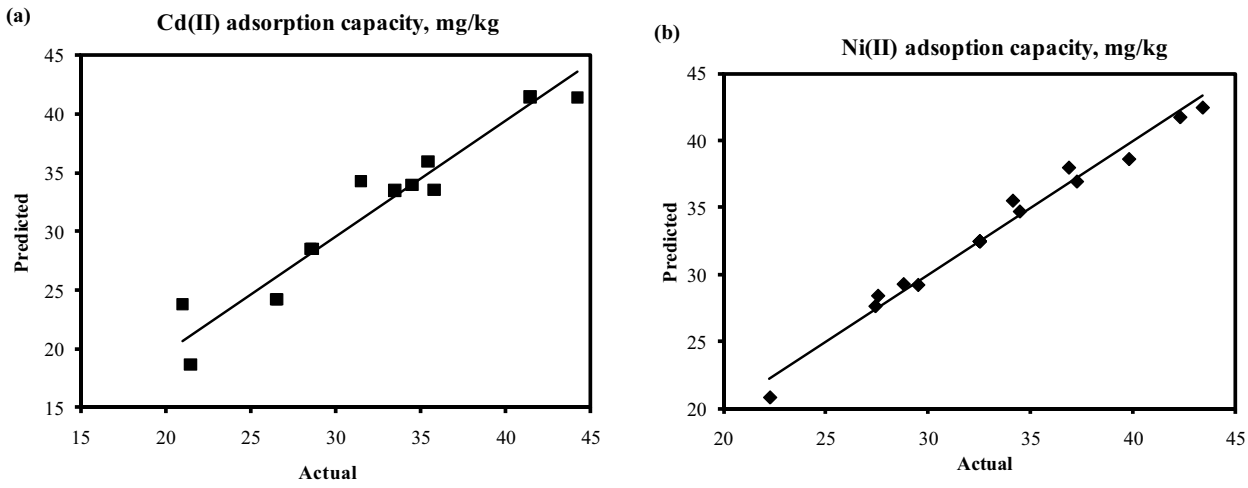

Fig. S3. Plot for the relationship between experimental and predicted value for (a) Cd(II) and (b) Ni(II) adsorption capacity.

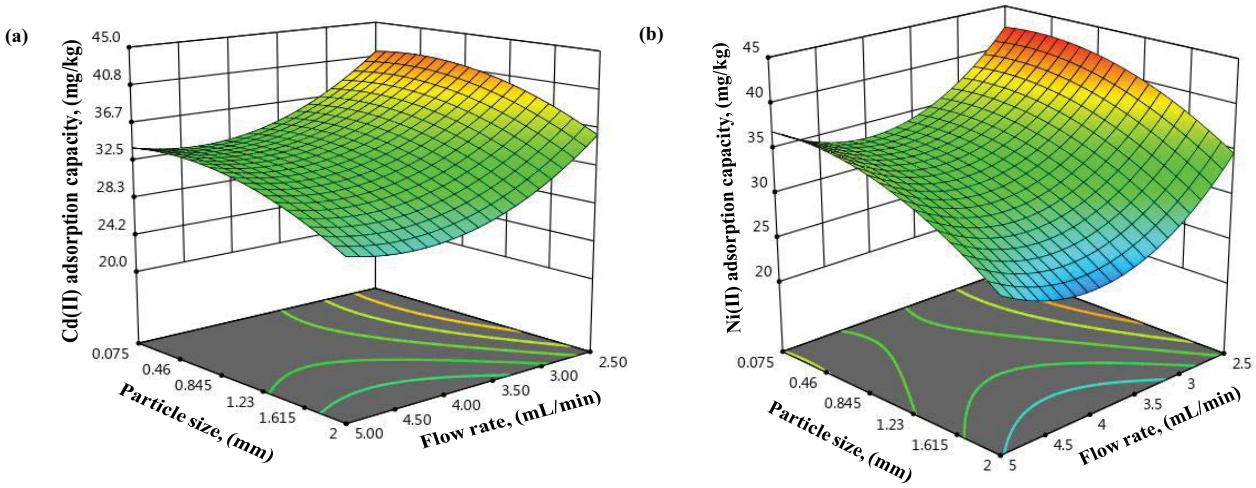

Fig. S4. Combined effect of flow rate and particle size on (a) Cd(II) and (b) Ni(II) adsorption capacity.